

**DETERMINATION OF THE PARTON DENSITIES OF THE
PROTON AND α_S AT HERA**

Leif Jönsson

(Representing the H1 and ZEUS collaborations)

Physics Department, University of Lund, Lund, Sweden

Abstract

The inclusive cross section for electron-proton scattering has been measured to a high degree of accuracy at HERA in order to investigate the structure of the proton. Recent measurements by the ZEUS experiment at values of x_{Bj} up to unity, as well as measurements with polarized lepton beams by H1 and ZEUS are discussed. The determination of the strong coupling constant from measurements of jets and from fits where the inclusive cross sections have been combined with additional data, to further constrain the parton density functions, is described.

1 Introduction

The proton structure functions have been extensively studied at the electron-proton collider HERA. The electron-proton scattering cross section can be obtained by convoluting the analytically calculable partonic cross section, σ_{pQCD} , with a parton density function (PDF), f_i , that provides the probability of scattering against a parton carrying a certain fraction x of the proton momentum.

$$\sigma = \left[\sum_{i=g,q,\bar{q}} \int dx f_i(x, \mu_f, \alpha_s(\mu_r)) \sigma_{pQCD}(x, \mu_f, \alpha_s(\mu_r)) \right] (1 + \delta_{had}) \quad (1)$$

The factorization scale μ_f defines at which value of the chosen scale the evolution stops, and μ_r is the renormalization scale, which is the scale variable used in the expansion of the strong coupling constant, α_s . The term δ_{had} takes the hadronization corrections into account.

The parton density function can not be calculated completely but the distribution at a starting scale μ_o has to be extracted experimentally. This is possible through measurements of the proton structure functions, which in leading order QCD are related to the parton density functions. In the quark-parton model (QPM) the inclusive double differential neutral current electron-proton cross section can be expressed in terms of three independent generalised structure functions, \tilde{F}_2 , \tilde{F}_L and $x\tilde{F}_3$, according to:

$$\frac{d^2\sigma_{NC}^{e\pm p}}{dx dQ^2} = \frac{2\pi\alpha^2}{xQ^4} \left[(1 + (1-y)^2)\tilde{F}_2(x, Q^2) - \frac{y^2}{2}\tilde{F}_L(x, Q^2) \mp (y - \frac{y^2}{2})x\tilde{F}_3(x, Q^2) \right] \quad (2)$$

with $\tilde{F}_L = \tilde{F}_2 - 2x\tilde{F}_1$ being the longitudinal structure function. The negative square of the boson four-momentum, Q^2 , also called the *virtuality*, is a measure of the resolution power of the exchanged boson. α is the fine structure constant, and y is the inelasticity of the process, defined in the proton rest frame as the energy fraction of the incoming electron transferred by the boson. The generalised structure functions \tilde{F}_2 and $x\tilde{F}_3$ can be decomposed into terms describing electromagnetic and weak interactions, and the interference between them, in the following way:

$$\tilde{F}_2^\pm = F_2 - (v_e \pm P_e a_e) \frac{\kappa Q^2}{(Q^2 + M_Z^2)} F_2^{\gamma Z} + (v_e^2 + a_e^2 \pm P_e 2v_e a_e) \left(\frac{\kappa Q^2}{Q^2 + M_Z^2} \right)^2 F_2^Z \quad (3)$$

$$x\tilde{F}_3^\pm = -(a_e \pm P_e v_e) \frac{\kappa Q^2}{(Q^2 + M_Z^2)} xF_3^{\gamma Z} + (2v_e a_e \pm P_e (v_e^2 + a_e^2)) \left(\frac{\kappa Q^2}{Q^2 + M_Z^2} \right)^2 xF_3^Z \quad (4)$$

where the different signs correspond to electron and positron scattering, respectively. The relative amount of Z and γ exchange is given by $\kappa^{-1} = 4 \frac{M_W^2}{M_Z^2} (1 - \frac{M_W^2}{M_Z^2})$, whereas v_e and a_e are the vector and axial-vector couplings of the electron to the Z^o . The lepton beam polarization is denoted P_e and the terms containing P_e express the parity violation.

The structure functions can be given in terms of the cross sections σ_T and σ_L , which correspond to the couplings to transversely and longitudinally polarized photons, respectively, and consequently $\sigma_{tot}^{\gamma P} = \sigma_L + \sigma_T$. At low Q^2 , the exchange of Z^o bosons is strongly suppressed compared to the photon exchange, and the cross section is therefore dominated by the contribution from F_2 (electromagnetic), which can be expressed as:

$$F_2(x, Q^2) = \frac{Q^2}{4\pi\alpha^2} (\sigma_L + \sigma_T) = \sum_q e_q^2 (xq(x) + x\bar{q}(x)) \quad (5)$$

i.e. the sum of the momentum weighted quark and antiquark densities, $xq(x)$ and $x\bar{q}(x)$, and the electromagnetic couplings to the photon given by the electric charge of the quarks.

The longitudinal structure function, \tilde{F}_L , describes the interaction with longitudinally polarized photons, which vanishes in zeroth order α_S processes due to

$$\tilde{F}_L(x, Q^2) = \frac{Q^2}{4\pi\alpha^2} \sigma_L \sim xg \quad (6)$$

with xg being the momentum weighted gluon distribution. From the ratio

$$R = \frac{\tilde{F}_L}{\tilde{F}_2 - \tilde{F}_L} = \frac{\tilde{F}_2 - 2x\tilde{F}_1}{2x\tilde{F}_1} = \frac{\sigma_L}{\sigma_T} \quad (7)$$

we get that $2x\tilde{F}_1 = \sigma_T$.

The structure function $x\tilde{F}_3(x, Q^2)$ is sensitive to the interference between photon and Z^o exchange as well as pure Z^o exchange, and is consequently only important at high Q^2 . The sign of the contribution from $x\tilde{F}_3$ to the cross section expression (eq.2) is different for e^-p - and e^+p scattering. Further, $x\tilde{F}_3^{\gamma Z}$ is sensitive to the difference in the quark and antiquark momentum distributions and can in leading order be written as:

$$x\tilde{F}_3^{\gamma Z} = 2x \sum_q (e_q a_q) (q - \bar{q}) = 2x(2u_v + d_v) \quad (8)$$

with u_v and d_v representing the valence quark distributions.

Via the relation to the PDF's the structure functions give us the probability to find a parton in the proton, carrying a fraction x of the proton momentum, if the probe has a resolution power Q^2 .

Intuitively one would expect that the probability of scattering against a pointlike parton would be independent of the momentum (resolution) of the probe. Thus, the structure function F_2 should not vary with Q^2 , a phenomenon called *scaling*. Experimental data from HERA have, however, clearly demonstrated that scaling is violated. This is related to the resolution power of the exchanged virtual photon in the sense that a high momentum photon is more sensitive to partons carrying a small momentum fraction than a low momentum photon. Since now the structure function depends on Q^2 and the strong coupling, α_S , the scaling violation effect can be used to extract the parton density function and the strength of the strong coupling.

The PDF's are determined through global fits to various experimental data at a smallest starting scale μ_o , at which perturbative calculations are still expected to be valid. Parton evolution equations can then be used to give the PDF at an arbitrary scale. Partonic activities below the starting scale are included into the starting distribution of the PDF.

HERA has measured the proton structure over a large kinematic range, covering almost five orders of magnitude in x_{Bj} and Q^2 . One of the most spectacular observations is the strong rise of $F_2(x, Q^2)$ at small x -values. In order to explore this kinematic region special efforts have been made, like:

- ▷ running HERA with the collisions point shifted in the direction of the proton beam
- ▷ running HERA with lower electron beam energy
- ▷ special analysis of events where the incoming electron has suffered from photon radiation

All this leads to an increased detector acceptance for events with lower Q^2 .

Due to the relation $Q^2 = x \cdot y \cdot s$, low Q^2 and very small x give access to high y , which is the region where σ_L makes a significant contribution to the cross section and thus F_L may be measured.

2 The high x -region

The high x -region has mainly been covered by previous fixed target experiments. The access to this region at HERA is restricted by acceptance limitations due to the fact that the scattered quark proceeds in the extreme forward direction, close to the beam pipe. Consequently, the jet produced is not well measured above a certain x -value that depends on Q^2 . ZEUS¹⁾ has used a new method to measure the neutral current cross section up to x -values of one, by determining the Q^2 value of the event from the scattered electron and the x -value from the reconstructed jet. If no jet with a transverse energy above 10 GeV was found by the longitudinally invariant k_t cluster algorithm, the event

was assigned to the x -bin not covered by the acceptance. Events with more than one jet were disregarded. The measured double differential cross section, $d^2\sigma/dxdQ^2$, was compared to predictions from Standard Model (SM) NLO calculations in which the CTEQ6M²⁾ parametrization of the proton PDF's were used. An overall good agreement between data and the SM predictions was observed although the theory tends to fall below data in the highest x -bin. These measurements will have a significant impact on the determination of the valence quark distributions in the high x -region.

3 Cross section measurements with polarized lepton beams

3.1 Polarization asymmetry

Longitudinally polarized electron beams, delivered by HERA since 2002, have been used to measure the neutral current cross section, which according to the SM should depend on the polarization of the incoming lepton. The degree of polarization is given by $P_e = (N_R - N_L)/(N_R + N_L)$, where N_R and N_L represents the number of right- and left handed leptons in the beam. The polarization effect is expected to be most significant at large Q^2 where Z^0 boson exchange becomes important and may be established by measuring the cross section asymmetry for right- and left handed $e^\pm p$ scattering, according to:

$$A^\pm = \frac{2}{P_R - P_L} \frac{\sigma^\pm(P_R) - \sigma^\pm(P_L)}{\sigma^\pm(P_R) + \sigma^\pm(P_L)} \quad (9)$$

where P_R and P_L stand for right- and lefthanded polarization, respectively. A^+ and A^- will have opposite signs due to the different signs of the $x\tilde{F}_3$ -term in the cross section expression (eq.2). The combined data from H1 and ZEUS on the asymmetries (A^\pm) as a function of Q^2 are shown in Fig.1 and are seen to be in good agreement with the SM predictions from QCD fits performed by H1 and ZEUS, respectively.

3.2 Determination of $x\tilde{F}_3$

A so called reduced cross section can be defined as:

$$\tilde{\sigma}^\pm(x, Q^2) = \frac{d^2\sigma_{NC}^\pm}{dxdQ^2} \frac{xQ^4}{2\pi\alpha^2} \frac{1}{Y_\pm} = \tilde{F}_2 \mp \frac{Y_-}{Y_+} x\tilde{F}_3 - \frac{y^2}{Y_+} \tilde{F}_L \quad (10)$$

where the helicity dependence is given by the terms $Y_\pm = 1 \pm (1 - y^2)$. The structure function $x\tilde{F}_3$ can be extracted from the difference in magnitude of the reduced cross sections for electron and positron scattering.

$$x\tilde{F}_3 = \frac{Y_+}{2Y_-} (\tilde{\sigma}^{e^-p} - \tilde{\sigma}^{e^+p}) \quad (11)$$

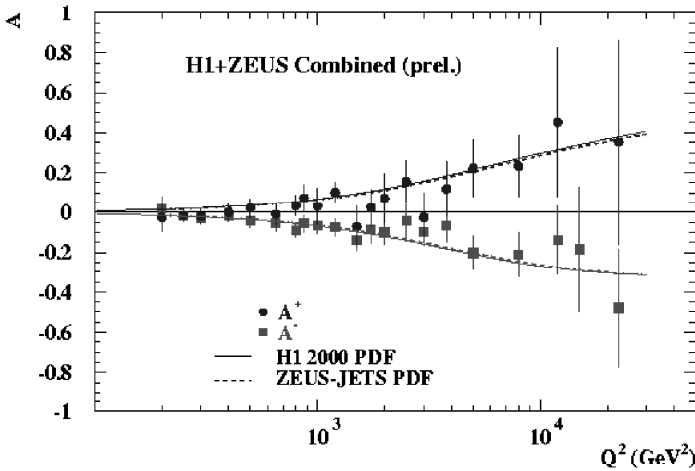


Figure 1: The Q^2 dependence of the cross section asymmetry A^\pm from combined H1 and ZEUS data. The curves represent SM QCD fits by H1 and ZEUS, respectively.

in which the dominant contribution comes from the γZ interference. Since $x\tilde{F}_3$ depends only slightly on Q^2 , the data from different Q^2 regions can be averaged by taking the weak Q^2 dependence into account. The results from H1 and ZEUS at an average Q^2 value of 1500 GeV² are shown in Fig.2. Data are reasonably well described, within the fairly large errors, by the NLO fits from both H1 ³⁾ and ZEUS ⁴⁾. These results contribute to constrain the valence quark distributions at low x_{Bj} .

4 Determination of the strong coupling constant

The following procedure is used to determine the value of the strong coupling constant, α_S . From a preselected parametrization of the proton parton density function, NLO calculations are performed for different values of $\alpha_S(M_Z)$. The $\alpha_S(M_Z)$ -dependence of the experimentally measured variable, denoted A , is parametrized according to:

$$\frac{d\sigma}{dA} = C_1\alpha_S(M_Z) + C_2\alpha_S^2(M_Z) \quad (12)$$

where C_1 and C_2 are parameters in a fit to the calculated $d\sigma/dA$ values at various $\alpha_S(M_Z)$.

The experimentally measured value of $d\sigma/dA$ is then converted to an $\alpha_S(M_Z)$ value via the fitted curve. The error in the measurement is translated into an error of $\alpha_S(M_Z)$ via the slope of the curve. Finally, the Renormalization

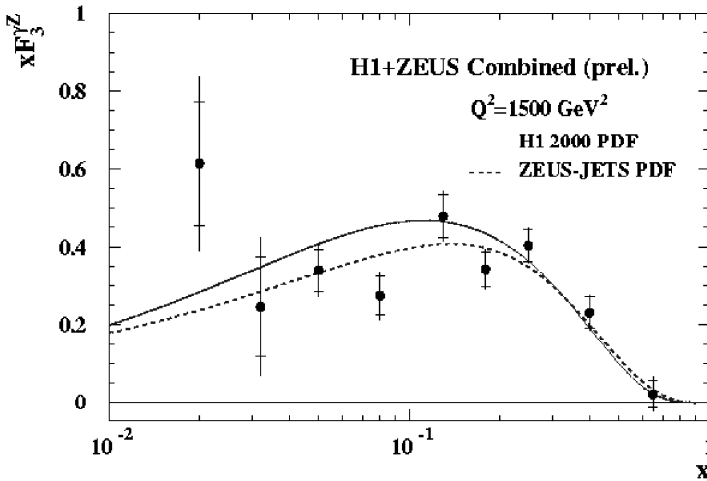


Figure 2: *The structure function $x F_3$ as a function of x at an average Q^2 value of 1500 GeV^2 from the H1 and ZEUS experiments.*

Group Equation (RGE) is used to extract the α_S values at different scales and thereby the running of the coupling can be established. By using different parametrizations of the PDF's the parton density function dependence may be estimated.

4.1 Measurement of α_S from inclusive jet production at high Q^2

A number of different observables have been measured in order to determine the strong coupling constant. For example the QCD predictions on jet production depend on both the PDF's and α_S . The measured cross sections can be used together with global fits of the proton PDF's to extract α_S . Jets from order α_S processes i.e. QCD-Compton and BGF, provide direct sensitivity to the strong coupling and enable precision tests of QCD. In the Breit frame jets from zeroth order scattering processes produce no transverse energy whereas in leading order processes (BGF or QCD-Compton) transverse jets may be observed.

The longitudinally invariant k_t algorithm ⁵⁾ is the most frequently used method for reconstructing jets in ep collision events. A cone in the pseudo-rapidity (η) - azimuthal (ϕ) space defines the jet radius as $R = \sqrt{\eta^2 + \phi^2}$. Most analyses so far have been performed with $R = 1$. It turns out that the inclusive jet production cross section provides the experimentally most precise determination of α_S . The ZEUS experiment ⁶⁾ has studied jet cross sections as a function of the jet radius in order to find an optimal value of R for which the NLO calculations provide the highest precision. Jet radii of $R = 0.5, 0.7$ and 1 have been used to study the Q^2 - and E_T -dependence of the jet cross

sections in events containing at least one jet with $E_T > 8$ GeV in the kinematic ranges $Q^2 > 125$ and > 500 GeV², respectively. The NLO calculations were performed by DISENT⁷⁾ in the \overline{MS} scheme with five flavours, using the ZEUS parametrization of the proton PDF's. The variation of the cross section over several orders of magnitude is well reproduced by the theory. A linear increase of the measured cross section with increasing R is observed and can be understood from the simple fact that more transverse energy is contained in the cone as it opens up, resulting in an increased number of jets exceeding the minimum E_T requirement. The theoretical uncertainties in the cross section integrated over the Q^2 range decreases in both cases slightly when going from $R = 0.5$ to 1, which is mainly attributed to higher order corrections and hadronization.

The H1 experiment has compared cross section measurements of inclusive jets in the Q^2 range 150 - 15000 GeV² with NLO calculations provided by the NLOJET++ program⁸⁾, in the \overline{MS} scheme with five massless quark flavours, using the CTEQ6.5M parametrization²⁾ of the proton PDF, and the value of the strong coupling constant has been extracted. The jets were reconstructed by the inclusive k_t algorithm provided they had a transverse momentum greater than 7 GeV. The cross sections as a function of Q^2 and E_T are well described by the NLO predictions within the dominating uncertainties given by the renormalization- and factorization scales. Twenty different measurements, subdivided into five Q^2 -bins, of the double differential inclusive jet cross section, $d^2\sigma/dQ^2dE_T$, are compatible with the predicted scale dependence of α_S . All the twenty measurements have been used in a combined fit from which the following value of $\alpha_S(M_Z)$ was obtained:

$$\alpha_S(M_Z) = 0.1187 \pm 0.0015(\text{exp.})_{-0.0037}^{+0.0052}(\text{theory})_{-0.0014}^{+0.0021}(\text{PDF}) \quad (13)$$

4.2 Determination of α_S from multi jet production at high Q^2

A measurement of the ratio between three and two jet event cross sections can be used to determine the value of the strong coupling constant, provided the cross sections can be measured with high enough precision. The advantage with this method is that the correlated systematic errors and the renormalization scale uncertainties cancel to a large extent while the disadvantage is the low statistics available. The H1 and ZEUS experiments have performed this analysis in the Breit frame over a wide kinematic range covering $10 < Q^2 < 15000$ GeV². Jets with $E_T > 5$ GeV, as reconstructed by the inclusive k_t algorithm, were used for the cross section measurements. In order to avoid problems with the phase space regions sensitive to infrared divergencies, the invariant mass of the jets with the highest transverse energies were required to be $M_{2jet} > 25$ GeV and $M_{3jet} > 25$ GeV, respectively. The reliability of the NLO calculations are thereby ensured. These calculations are performed by

the NLOJET++ program in the \overline{MS} scheme for five massless quark flavours and with various parametrization of the proton PDF. The Q^2 dependence of the measured cross sections and consequently of the ratio $R_{3/2}$ is in good agreement with the predictions of NLOJET++ in the phase space region where the electroweak effects can be neglected.

From fits to the measured ratios $R_{3/2}$, values of $\alpha_S(M_Z)$ were determined in five different Q^2 bins, but also in the complete Q^2 -region giving the results below.

H1:

$$\alpha_S(M_Z) = 0.1175 \pm 0.0017(stat.) \pm 0.0050(syst.)_{-0.0068}^{+0.0054}(theory) \quad (14)$$

ZEUS:

$$\alpha_S(M_Z) = 0.1179 \pm 0.0013(stat.)_{-0.0046}^{+0.0028}(exp.)_{-0.0046}^{+0.0064}(theory) \quad (15)$$

4.3 Combined fits of α_S and the gluon density

Measurements of the Q^2 dependence of the structure function (scaling violation) provided by inclusive cross section measurements is the most commonly used method to determine the PDF's via the DGLAP evolution equations. However, fits to the inclusive cross sections alone suffer from strong correlations between the shape of the parton distribution and α_S . These correlations may be reduced by including data which constrain the PDF's in an independent and complementary way.

Recent measurements of the structure function $F_2(x, Q^2)$ at low Q^2 , performed by the H1 and ZEUS experiments, provide a considerable improvement compared to previous measurements. The kinematic range covered, $1.5 < Q^2 < 150 \text{ GeV}^2$ and $3 \cdot 10^{-5} < x < 0.2$, means an extension in x such that an overlap with previous fixed target data is obtained. In spite of this the precision of these data together with previous HERA data at large x and high Q^2 is not sufficient to give enough constraints of both the gluon density and α_S to allow for a simultaneous determination. Instead the low x data from H1, which essentially constrain the gluon distribution, have been combined with large x data provided by the BCDMS μp scattering experiment, in order to reduce the strong correlation between α_S and the gluon distribution, $xg(x, Q^2)$, and thereby enable an accurate simultaneous determination of the two.

The structure function $F_2(x, Q^2)$ has been decomposed into the gluon distribution, $xg(x, Q^2)$, and two independent parton density functions, one of which is defining the valence quark distribution whereas the other constrains the sea-quark distribution and provides a small valence quark correction in order to describe the low x behaviour of F_2 . The x dependence of these parton distribution functions have been parametrized at a smallest scale Q_o^2 of 4 GeV^2 .

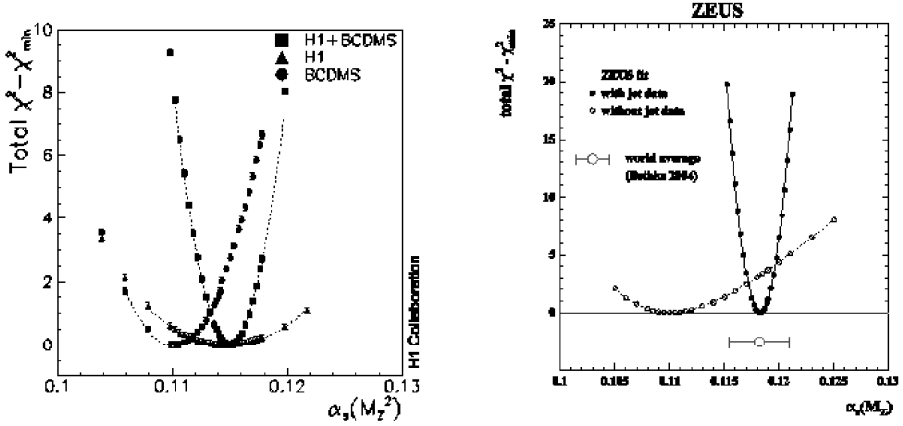


Figure 3: The χ^2 profiles as a function of $\alpha_s(M_Z)$ for a NLO DGLAP fit using the H1 ep and BCDMS μp data (left) and the ZEUS data with and without the jet data included (right).

In a NLO QCD fit to the combined H1 and BCDMS data, α_s is left as a free parameter, resulting in a value:

$$\alpha_s(M_Z^2) = 0.1150 \pm 0.0017(\text{exp.})_{-0.0005}^{+0.0009}(\text{model}) \quad (16)$$

The fit to the data implies the minimization of a χ^2 function, taking correlations between data points caused by systematic uncertainties into account. The results of the fits are shown in Fig.3(left).

The ZEUS experiment has performed a simultaneous fit to $\alpha_s(M_Z)$ and the proton PDF's in an analysis which includes neutral and charged current inclusive DIS cross sections from e^+p and e^-p scattering together with jet data. Two different jet samples were used in the fit. On one hand the DIS inclusive jet cross sections as a function of the transverse jet energy, E_T , in the Breit frame, for different Q^2 bins were included. On the other hand dijet cross sections in photoproduction as a function of E_T of the most energetic jet, as measured in the laboratory system, for different rapidity regions were also considered. A parametrization of the PDF's at a smallest scale $Q_0^2 = 7 \text{ GeV}^2$ provides a good fit of the jet cross sections over several orders of magnitude. The quality of the fit demonstrates that NLO QCD is able to simultaneously describe inclusive cross sections as well as jet cross sections.

The strong correlation between the gluon shape and the value of $\alpha_s(M_Z)$, which affects the fits to inclusive cross section data alone, is avoided by including the jet data, since their cross sections depend on the gluon PDF and the value of $\alpha_s(M_Z)$ in a different way compared to the total cross section. An

advantage in using different data sets from the same experiment compared to combining data from different experiments is that the contributions from correlated errors and normalization uncertainties are significantly reduced. The combined fit results in an α_S value of:

$$\alpha_S(M_Z) = 0.1183 \pm 0.0028(\text{exp.}) \pm 0.0008(\text{model}) \quad (17)$$

The χ^2 profile as a function of α_S , shown in Fig.3(right), illustrates the improved accuracy in the α_S determination from the data sample including the jet data compared to using the inclusive cross sections alone.

Fig.4 gives a compilation of various measurements of $\alpha_S(M_Z)$ at HERA. Within uncertainties all these results agree internally and with the world average.

$$\alpha_S(M_Z) = 0.1189 \pm 0.0010 \quad (18)$$

In Fig.5 the HERA results are complemented with measurements by other experiments to illustrate the running of α_S with the energy scale Q . The Q dependence of α_S is well reproduced by QCD predictions, which makes it relevant to extrapolate all results to a common scale defined by the rest mass of the Z^0 boson, M_Z , using the Renormalization Group Equation.

5 Summary

A measurement of the inclusive ep -cross section in the high x_{Bj} region by the ZEUS experiment is well described by recent parametrizations of the parton density function, except for the highest x_{Bj} -bin where the predictions under-shoot the data. The first measurements from the H1 and ZEUS experiments with polarized lepton beams at HERA give cross sections which are consistent with the predictions of the Standard Model and the observed asymmetry clearly demonstrates the parity violation at small distances. The structure function $xF_3^{\gamma Z}$, which can be extracted from the polarization cross section asymmetries, is sensitive to the valence quark distributions and turns out to be in good agreement with Standard Model predictions.

The cross section of inclusive jet production as measured by the H1 and ZEUS experiments is well reproduced by NLO QCD calculations and fits to the data have been used to extract $\alpha_S(M_Z)$ and to demonstrate the scale dependence of the coupling constant. The ratio between trijet and dijet cross sections is also well described by NLO calculations over the measured Q^2 range where electroweak effects can be neglected. The strong coupling can be extracted with a precision that profits from cancellations of systematic errors. The inclusive cross section measurements have been combined with other data in order to further constrain the parton density functions and to extract $\alpha_S(M_Z)$ in combined fits. All results on $\alpha_S(M_Z)$ presented, are consistent and in good agreement with the world average value.

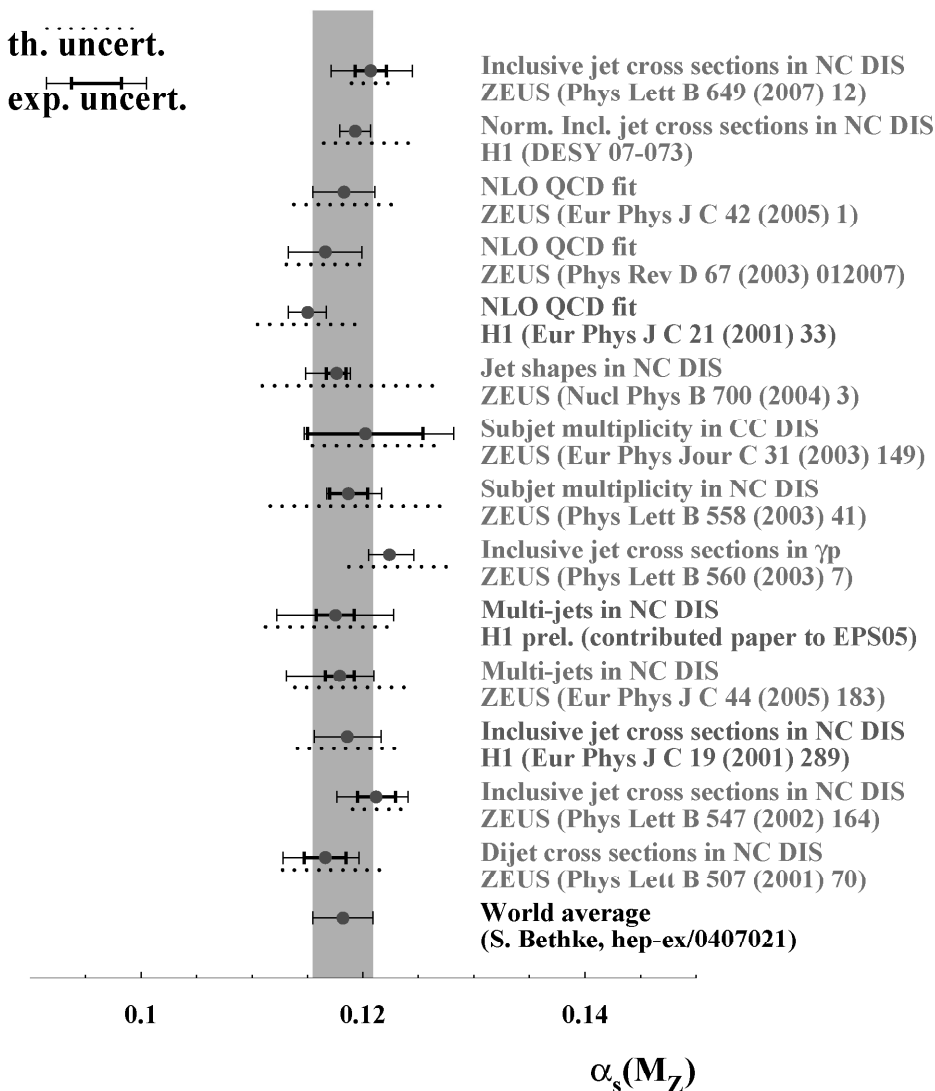


Figure 4: A compilation of $\alpha_s(M_Z)$ measurements at HERA compared to the world average value.

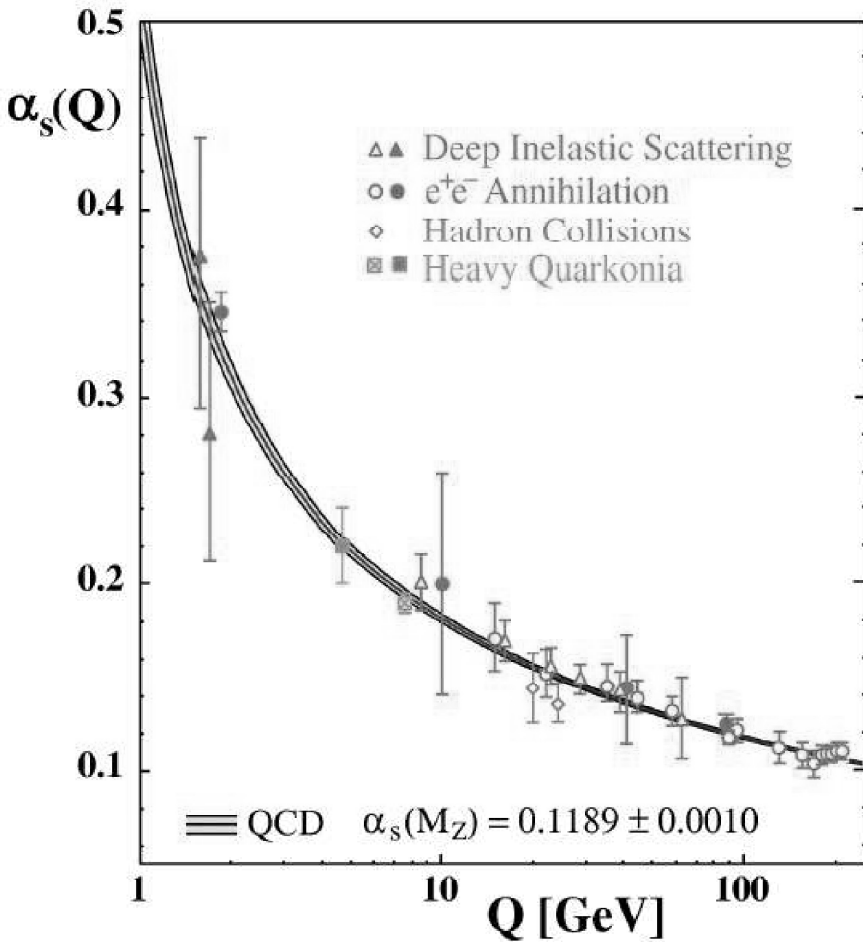


Figure 5: *The scale dependence of $\alpha_s(Q)$ including data from various measurements compared to the QCD prediction.*

6 Acknowledgements

I would like to thank the organizers for an enjoyable and interesting conference. Colleagues from H1 and ZEUS are acknowledged for help with the material of this presentation.

References

1. ZEUS Collaboration, S. Chekanov *et al*, Eur. Phys. J. **C49**, 523 (2007).
2. J. Pumplin *et al*, JHEP **0207**, 012 (2002).
3. H1 Collaboration, C. Adloff *et al*, Eur. Phys. J. **C30**, 1 (2003).
4. ZEUS Collaboration, S. Chekanov *et al*, Phys. Lett. **B637**, 210 (2006).
5. S. Catani *et al*, Nucl. Phys.**B406**, 187 (1993).
6. ZEUS Collaboration, S. Chekanov *et al*, hep-ex/0701039
7. S. Catani and M. Seymour, Nucl. Phys.**B485**, 291 (1997).
8. Z. Nagy and Z. Trocsanyi, Phys. Rev. Lett. **87**, 082001 (2001).
9. ZEUS Collaboration, S. Chekanov *et al*, Eur. Phys. J. **C44**, 183 (2005).